Adaptor bypass mutations of *Bacillus subtilis spxA* suggest a mechanism for YjbH-enhanced proteolysis of the regulator Spx by ClpXP

Chio Mui Chan Erik Hahn and Peter Zuber

Supplemental material

Supplementary Tables

TableS1. *Bacillus subtilis* strains and plasmids used in this study

Strains or plasmids	Relevant genotype or properties	Reference
Strains		
ORB7852	*trpC2 pheA1 spx*::*neo yjbH*::tet^{F}	(Kommineni *et al*., 2011)
ORB8729	*trpC2 pheA1 spx*::*neo yjbH*::*tet*^{F} *amyE*:: $P_{hyspank}$-*spx(wt)*	
ORB8731	*trpC2 pheA1 spx*::*neo yjbH*::*tet*^{F} *amyE*:: $P_{hyspank}$-*spx(F113A)*	
ORB8732	*trpC2 pheA1 spx*::*neo yjbH*::*tet*^{F} *amyE*:: $P_{hyspank}$-*spx(L114A)*	
ORB8750	*trpC2 pheA1 rpoA(cxs-1,Y263C) spx*::*neo yjbH*::*tet*^{F} *amyE*:: $P_{hyspank}$-*spx(WT)*	
ORB8752	*trpC2 pheA1 rpoA(cxs-1,Y263C) spx*::*neo yjbH*::*tet*^{F} *amyE*:: $P_{hyspank}$-*spx(F113A)*	
ORB8753	*trpC2 pheA1 rpoA(cxs-1,Y263C) spx*::*neo yjbH*::*tet*^{F} *amyE*:: $P_{hyspank}$-*spx(L114A)*	
ORB8968	*trpC2 pheA1 spx*::*neo yjbH*::*tet*^{F} *amyE*:: $P_{hyspank}$-*spx(F113A), clpX*::*erm*	
Plasmids		
pET23a	Protein expression vector with C-terminal His_6 tag	
pPROEX-1	Protein expression vector with cleavable N-terminal His_6 tag by γTEV (tobacco etch virus) protease	
pDG646	Source of erythromycin resistance cassette	
pDR111	*amyE* integration vector with $P_{hyspank}$ promoter	
pSN17	pPROEX-1 derivative encoding N-terminal His6-tagged Spx.	
pEC-27	pPROEX-1 with AbrB with SFQLREAQRLAN at its C-terminus (Spx C-terminus last 12 a.a.)	
pEC-31	pPROEX-1 with AbrB with GYNEDEIRRFLPRKVRSFQLREAQRLAN at its C-terminus (Spx C-terminus last 28 a.a.)	
pEC-33	pPROEX-1 with *spx(R112A)*	
pEC-35	pPROEX-1 with *spx(R111A/R112A)*	
pEC-53	pDR111 with *spx(wt)*	
pEC-56	pPROEX-1 with *spx(F113A)*	
pEC-57	pPROEX-1 with *spx(I110A)*	
pEC-58	pPROEX-1 with *spx(L114A)*	
pEC-59	pPROEX-1 with *spx(P115A)*	
pEC-61	pDR111 with *spx(F113A)*	
pEC-62	pDR111 with *spx(L114A)*	
pEC-66	pDG646 with *clpX (166-800)*	
pAL-108	pDR111 with *spx(R112A*^{DD}*)*	
pAL-109	pDR111 with *spx(R111A/R112A*^{DD}*)*	

Table S2. Primers

Primer	Sequence

EC35	TAGGCCATATGTTTATGAAATCTACTGGTATTGTAC
EC36	TAGGCGCGGCCGCTCAGTTTGCCAAACGCTGTGCTTCTCTTAATTGGAAAGATTTAAGGTTTTGAAGCTGGTTTT
EC40	TAGGCGCGGCCGCTTAGTTTGCCAAACGCTGTGCTTCTCTTAATTGGAAAGAGCGAACTTTTCTTTTAAGGTTTTGAAGCTGGTTTT
EC41	TAGGCGCGGCCGCTTAGTTTGCCAAACGCTGTGCTT
EC42	AAAACCAGCTTCAAAACCTTAAAGGATATAACGAAGACGAAATCA
EC43	TGATTTCGTCTTCGTTATATCCTTTAAGGTTTTGAAGCTGGTTTT
EC64	TAGGCGCTAGCTTAGTTTGCCAAACGCTGTGCTT
EC78	TAGGGAAGCTTAGAGAACAAGGAGGAGTAGTCACATGGTTACACTATACACATCAC
EC79	AACGAAGACGAAGCCAGACGTTTCCTG
EC80	CAGGAAACGTCTGGCTTCGTCTTCGTT
EC81	CGAAATCAGACGTGCCCTGCCAAGAAAA
EC82	TTTTCTTGGCAGGGCACGTCTGATTTCG
EC83	AATCAGACGTTTCGCGCCAAGAAAAGTTC
EC84	GAACTTTTCTTGGCGCGAAACGTCTGATT
EC85	AGACGTTTCCTGGCAAGAAAAGTTCGC
EC86	GCGAACTTTTCTTGCCAGGAAACGTCT
EC90	TAGGCTCTAGAGTAGAATTTAAAGACGTACCAAAG
EC91	TAGGCTCTAGACCGAATCCAATCACTTTTTGCG
o-sn01-6	GGGAATTCCATATGGTTACACTATACACATC
o-sn01-7	CGCGGATCCTTAGTTTGCCAAACGCTGTG

847
848

Supplementary figure legends

Fig. S1. Sequence alignment of Spx from *B. subtilis* and *Geobacillus thermodenitrificans*. The conserved residues are boxed, with completely conserved residues in magenta, identical residues in yellow, similar residues in cyan, and different residues in white.

Fig. S2. . *In vitro* Ni affinity pull-down experiments to detect interaction between *Gt*YjbH-His_6 and AbrB16 or AbrB28. Binding reactions contained 2.5 μM of each protein, and were incubated at room temperature for 10 min. M, marker; I, input; W, wash; E, elution (Experimental Procedures for details). C, contaminating protein in AbrB16 preparation.

Fig. S3. *In vitro* proteolysis assay of AbrB12, AbrB16, and AbrB28 in the absence of *Gt*YjbH-His_6. AbrB12, AbrB16, or AbrB28 (8 μM), ClpX (3 μM), and ClpP (8 μM) with an ATP-generating system (creatine kinase) were incubated at 37 °C for the times (min) indicated (left). Plots of AbrB12, AbrB16, and AbrB28 band intensities against time of reaction in separate experiments are shown. The intensities of ClpP protein in each lane were used as internal controls (Zhang & Zuber, 2007). The Spx/ClpP ratio in 0-min time point is defined as 100%. Below the graphs are SDS-polyacylamide gel images after Coomassie blue staining

showing bands of AbrB chimeric protein from samples of ClpXP proteolysis reactions.

Fig. S4. Purification of SpxF113A.

A. SDS- PAGE shows analyses of SpxF113A samples. UI: uninduced cells; I: induced cells with IPTG; S, P, supernatant and pellet (after French press and centrifugration), respectively.

B. SDS- PAGE shows SpxF113A Ni-NTA column eluants through denaturation-renaturation procedure.

Fig. S5. *In vitro* transcription of linear *trxB* (60 nt) with additions of Spx variants. 1, no Spx; 2, SpxWT; 3, His-SpxWT; 4, His-SpxR112A; 5, His-SpxR111A/R112A; 6, His-SpxI110A; 7, His-SpxF113A; 8, His-SpxL114A; 9, His-SpxP115A.

Fig. S6. Interaction of His_6-Spx with GtYjbH before and after denaturation/renaturation. Wild Spx with an N-terminal His_6 tag was subjected to denaturation and on-column renaturation according to the procedure described in materials and methods, except that soluble His_6-Spx was diluted in 10 vols. of denaturation solution (Experimental procedures) before application to the Ni-NTA column. Renaturation and interaction assays were conducted as described in Experimental procedures. A. Interaction of His_6-Spx or denatured and renatured His_6-Spx with GtYjbH. B. GtYjbH only applied to Ni-NTA column, confirming no

893 interaction of GtYjbH with Ni-NTA column. I: input; FT: flow-through; W: wash
894 fraction; E: elution.
895
896 **Fig. S7.**
897 **A .** A plot of Spx (WT, F113A, and L114A) band intensities against time of
898 chloramphenicol treatment is shown in the graph (From Fig. 5A). The intensities
899 of a protein recognized by anti-Spx antiserum in each lane were used as internal
900 controls. The Spx intensity normalized by 0-min time point is defined as 100%.
901
902 **B.** A plot of Spx (F113A) band intensities against time of chloramphenicol
903 treatment is shown in the graph (From Fig. 5B). The Spx intensity normalized by
904 0-min time point as described Fig.5 is defined as 100%.
905
906 **Fig. S8.** Immunoblot analysis of ClpX level using anti-ClpX antiserum in cells
907 bearing the $P_{hyspank}$- *spx (wt, F113A, or P114A)* in *yjbH* and *spx* null mutant and
908 in either *rpoA*$^+$ ($RNAP_{wt}$) or *rpoAY263C* ($RNAP_m$) genetic backgrounds. Cells
909 were grown to mid-exponential phase, induced with 1 mM IPTG for 1 hr, and
910 followed by 0.1 μg/μl chloramphenicol treatment as indicated in the figure.
911
912
913

Fig. S1

Sequence alignment of *Bacillus subtilis* and *Geobacillus thermodenitrificans* Spx

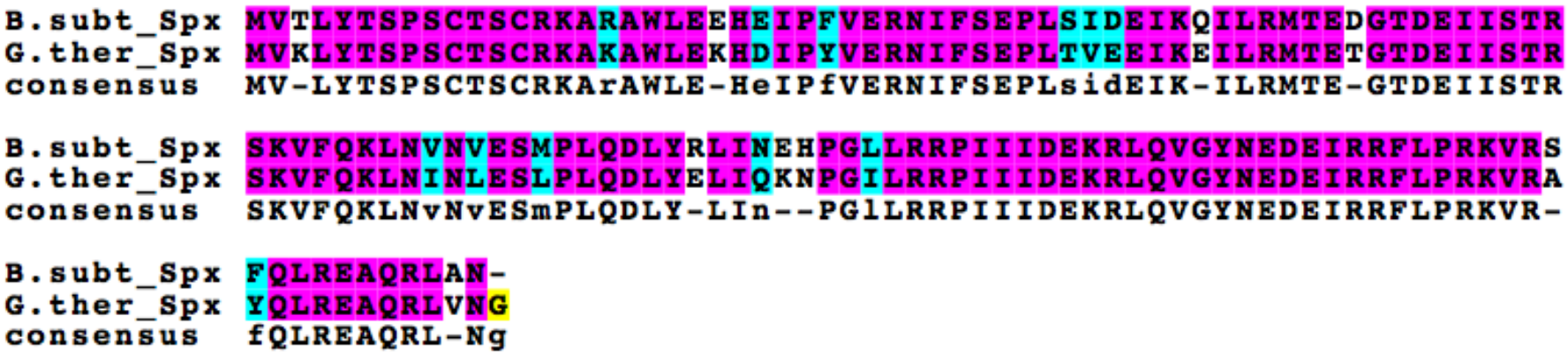

Fig. S2

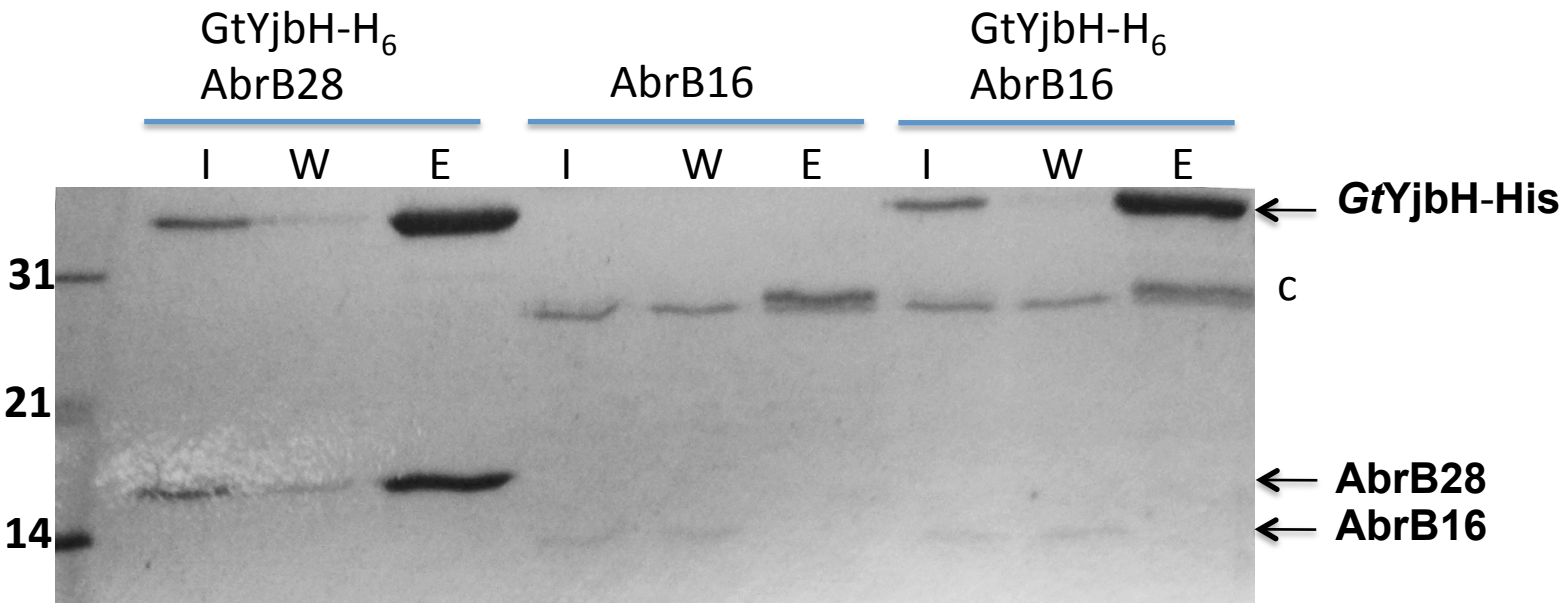
GtYjbH-H6
AbrB28
AbrB16
GtYjbH-H6
AbrB16
I
W
E
I
W
E
I
W
E
31
21
14
GtYjbH-His
c
AbrB28
AbrB16

Fig. S3

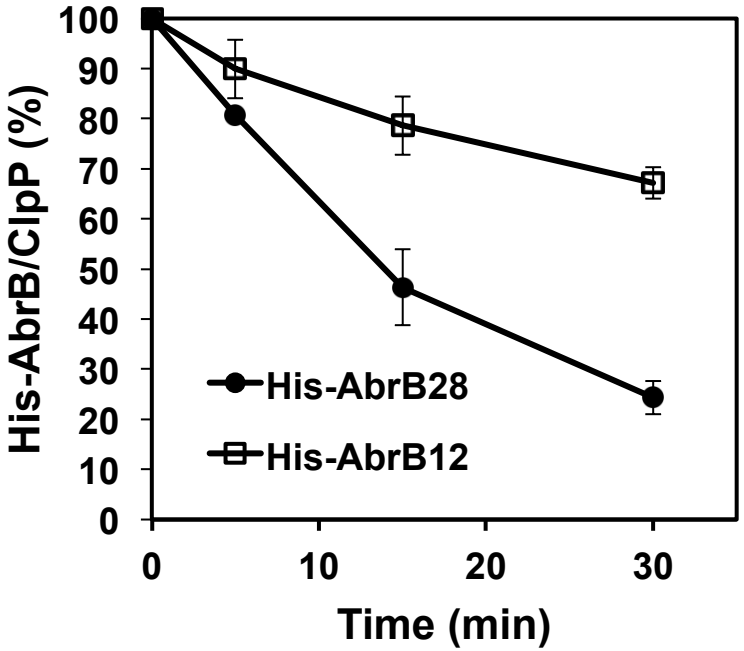
His-AbrB/ClpP (%)
100
90
80
70
60
50
40
30
20
10
0
0
10
20
30
Time (min)
His-AbrB28
His-AbrB12

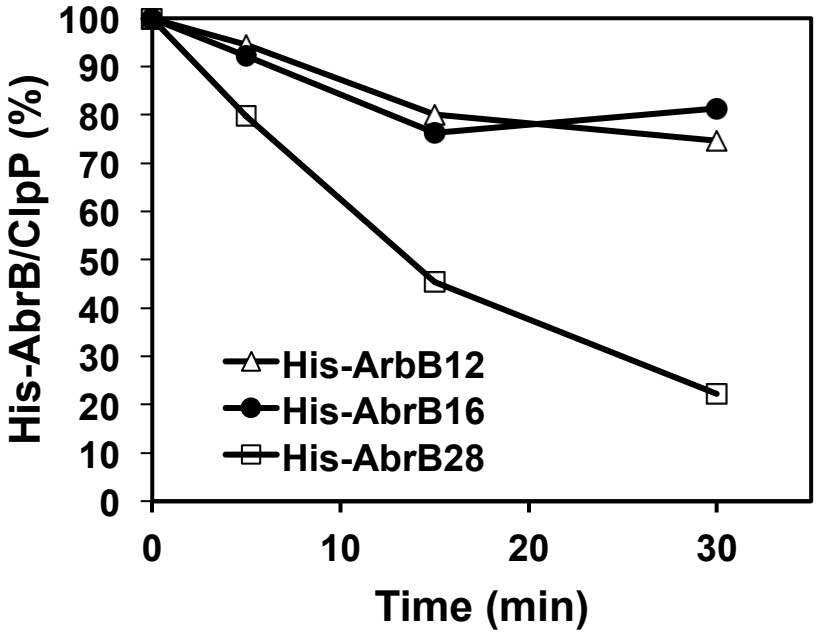
His-AbrB/ClpP (%)
100
90
80
70
60
50
40
30
20
10
0
0
10
20
30
Time (min)
His-ArbB12
His-AbrB16
His-AbrB28

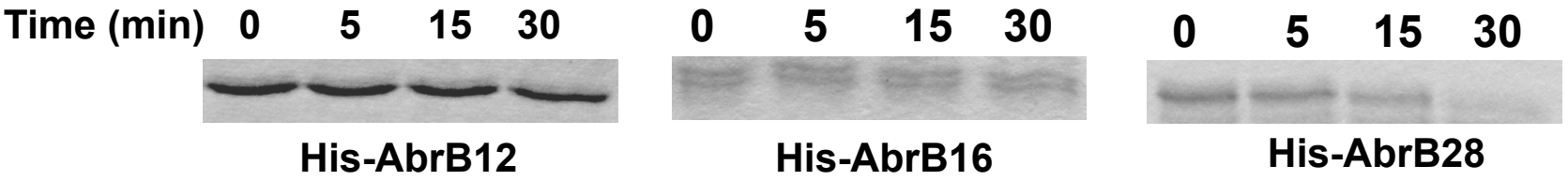
Time (min) 0 5 15 30
His-AbrB12
0 5 15 30
His-AbrB16
0 5 15 30
His-AbrB28

Fig. S4

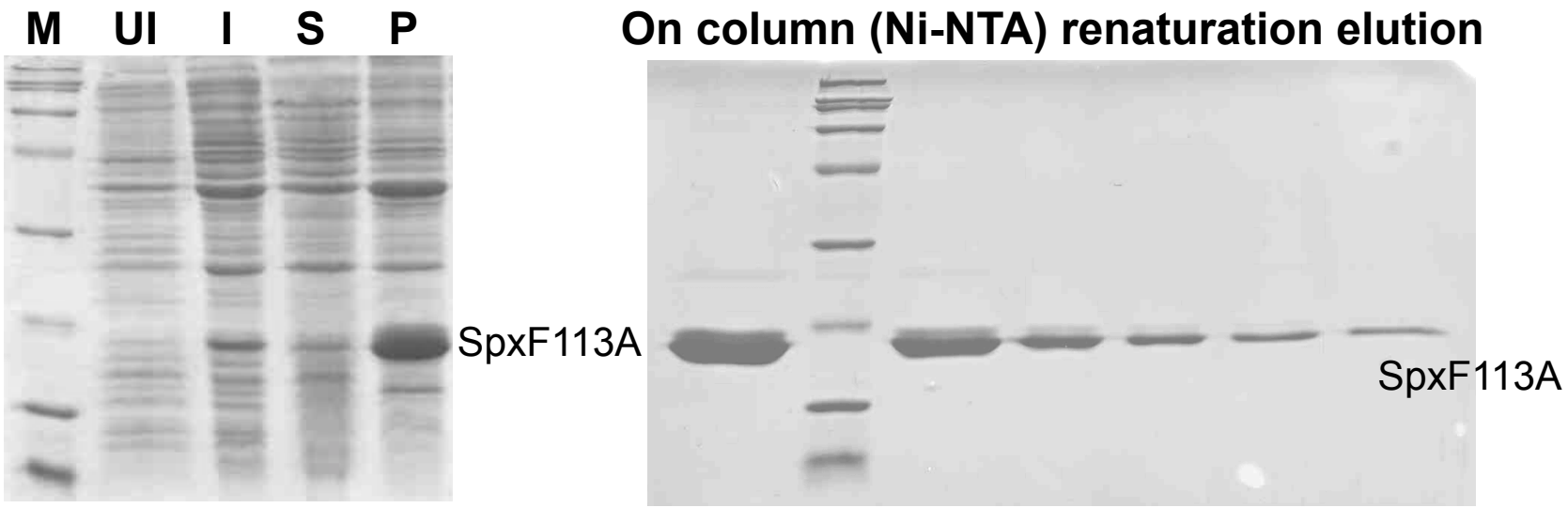
M
UI
I
S
P
SpxF113A
On column (Ni-NTA) renaturation elution
SpxF113A

Fig. S5

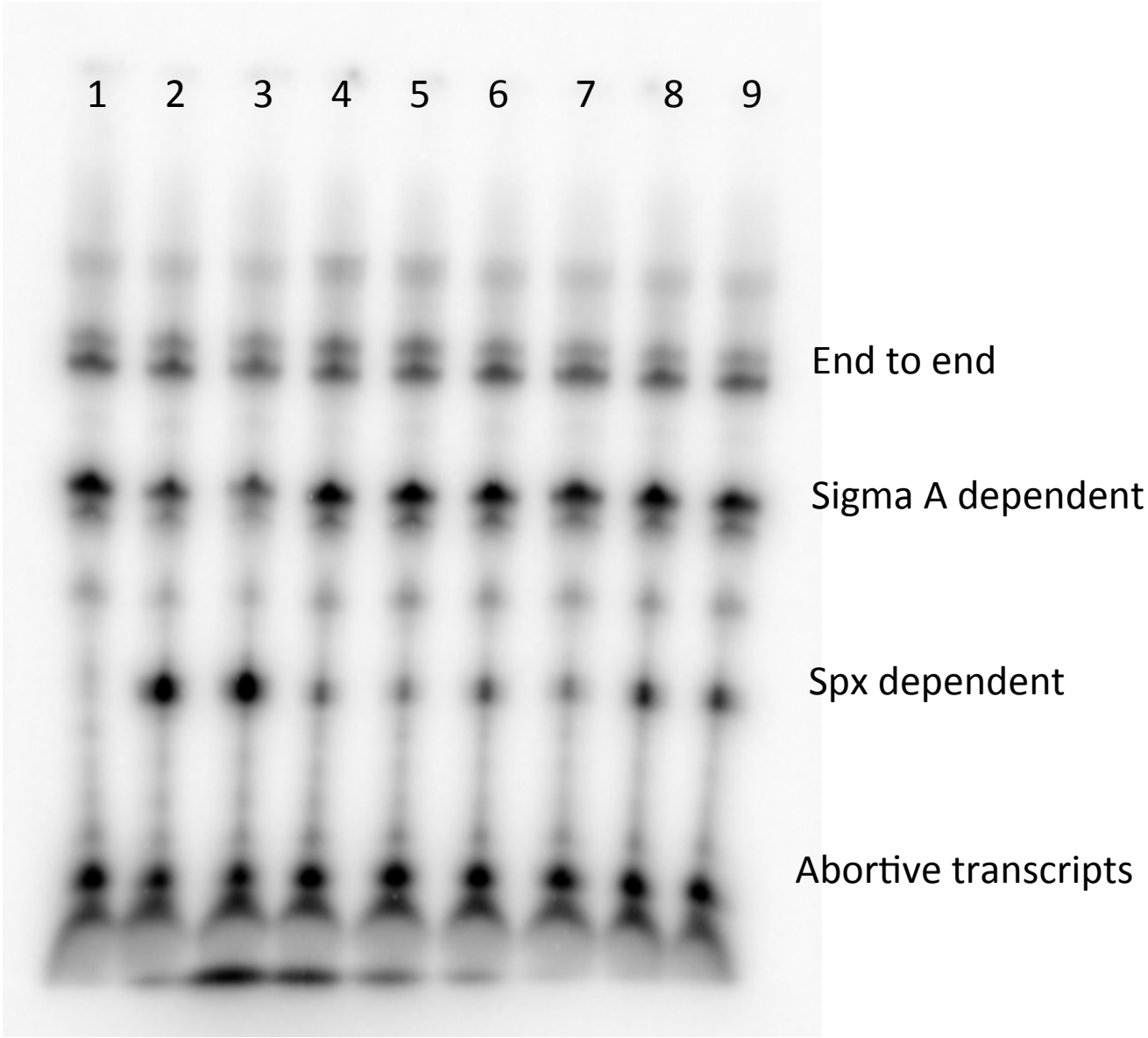
1
2
3
4
5
6
7
8
9
End to end
Sigma A dependent
Spx dependent
Abortive transcripts

Fig. S6

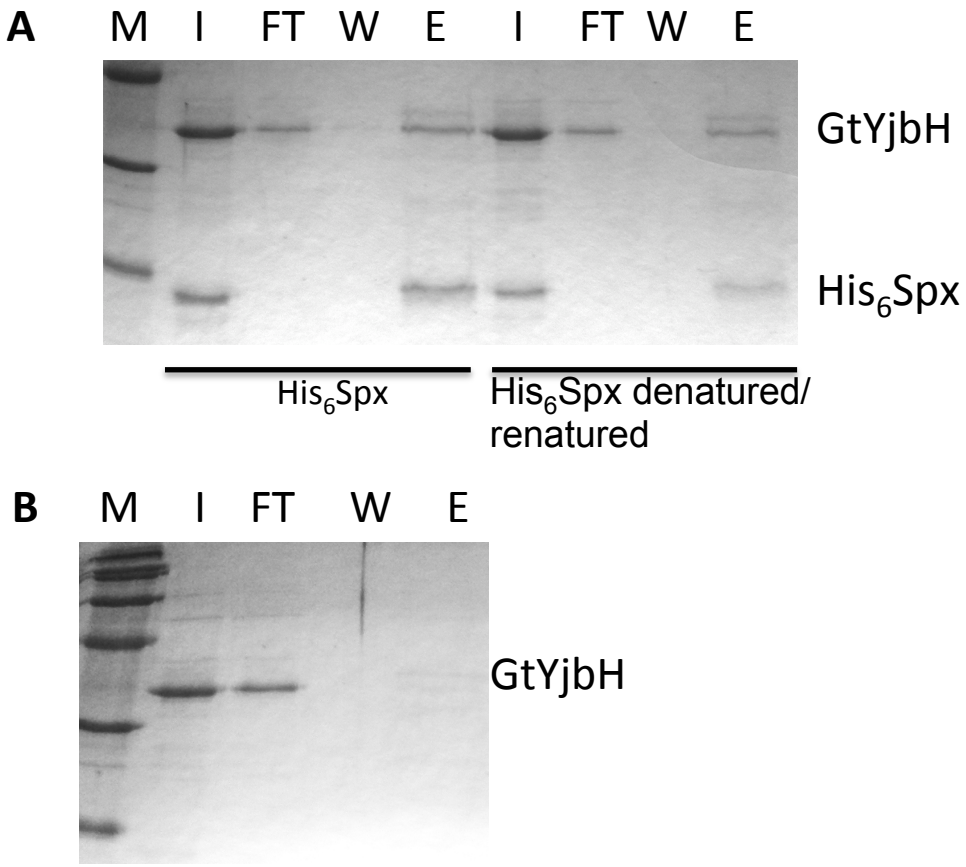
A
M I FT W E I FT W E
GtYjbH
His6Spx
His6Spx
His6Spx denatured/
renatured
B
M I FT W E
GtYjbH

Fig. S7

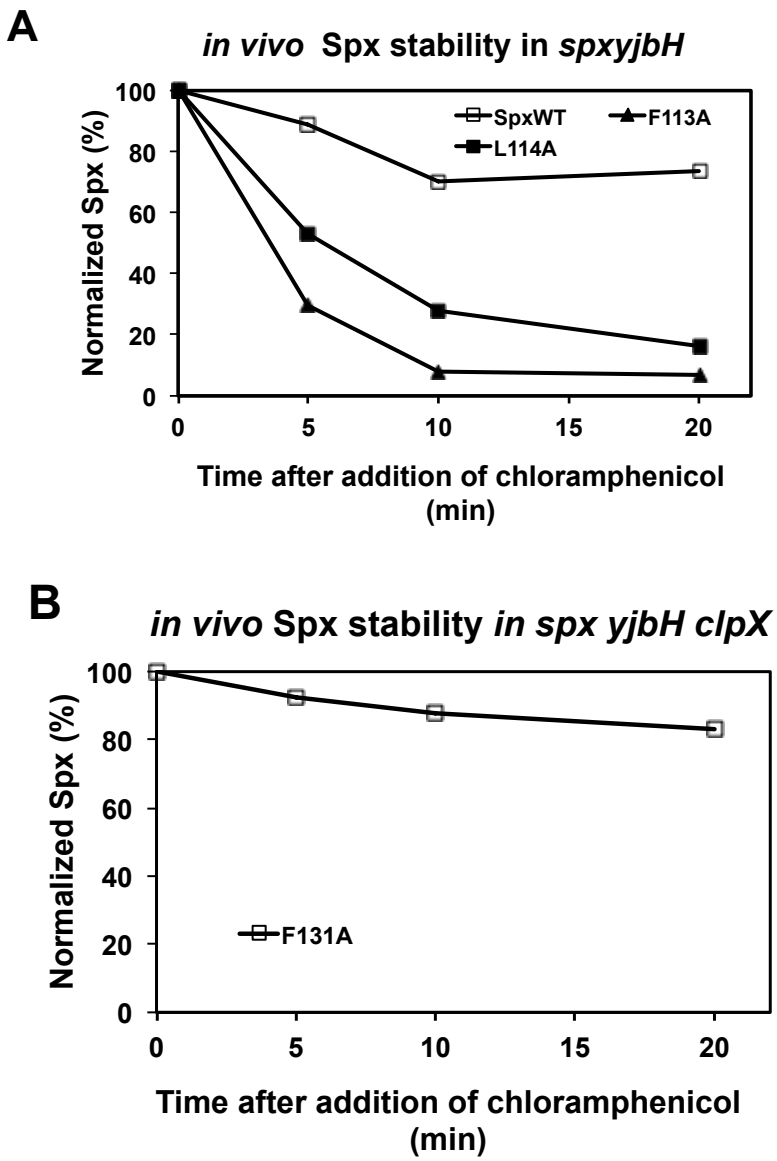
A
in vivo Spx stability in spxyjbH
Normalized Spx (%)
100
80
60
40
20
0
0
5
10
15
20
Time after addition of chloramphenicol (min)
SpxWT
F113A
L114A
B
in vivo Spx stability in spx yjbH clpX
Normalized Spx (%)
100
80
60
40
20
0
0
5
10
15
20
Time after addition of chloramphenicol (min)
F131A

Fig. S8

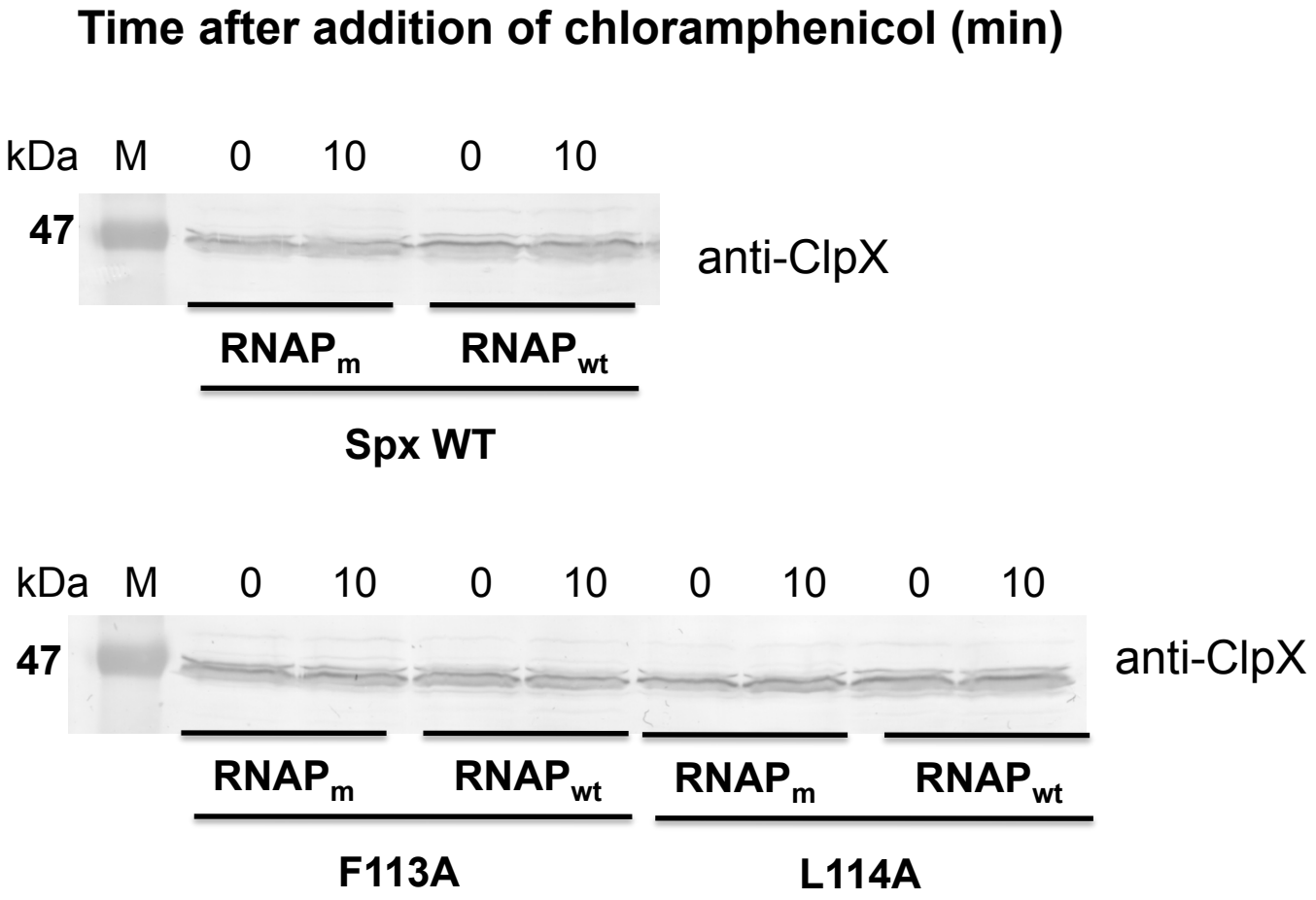
Time after addition of chloramphenicol (min)
kDa
M
0
10
0
10
47
anti-ClpX
RNAP$_m$
RNAP$_{wt}$
Spx WT
kDa
M
0
10
0
10
0
10
0
10
47
anti-ClpX
RNAP$_m$
RNAP$_{wt}$
RNAP$_m$
RNAP$_{wt}$
F113A
L114A